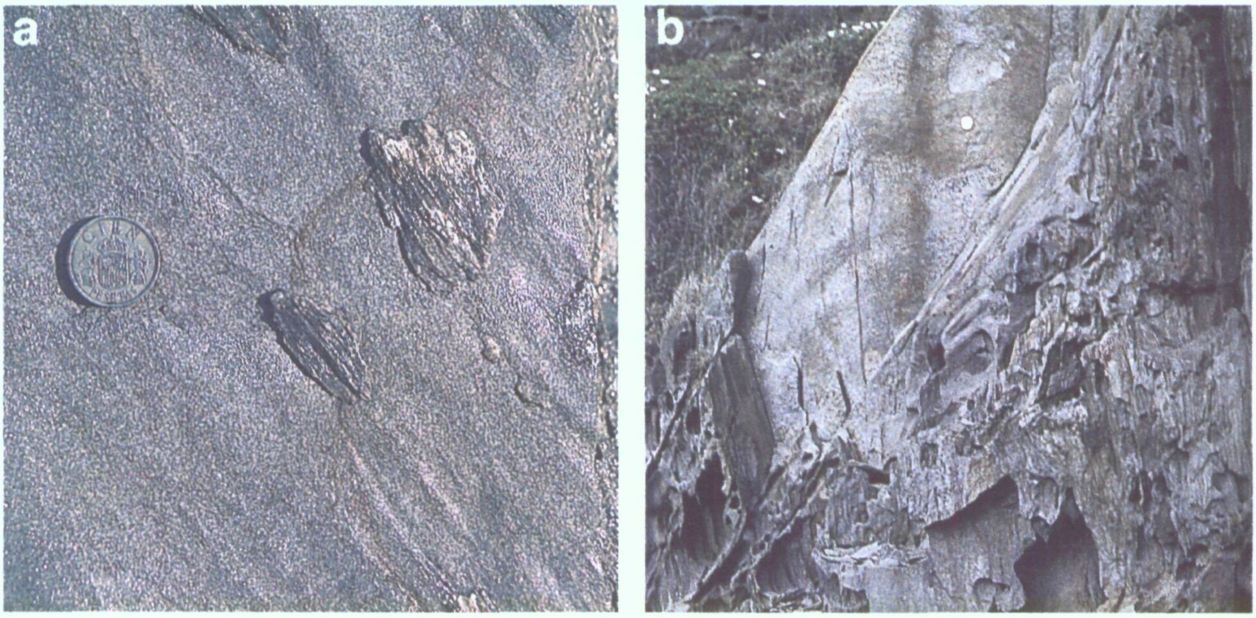

Fig. 41. Field photographs. (a): Steeply plunging L_2 mineral lineation defined by sillimanite, Club Mediterranée. (b): Sub-vertical L_2 crenulation lineation parallel to F_2 fold axis, south Cala Culip.

Microstructures

At the microscopical scale, D_2 structures are well displayed by (i) crenulations and development of polygonal arcs of recrystallized early micas and (ii) the axial planar growth of new phyllosilicates (Fig. 42a, b).

In regard to the porphyroblasts, they grow over S_1 foliation (Fig. 42c,d) developing inclusion patterns. S_1 is generally deflected around them but also is continuous inside them with straight inclusion patterns (S_i). Most porphyroblasts have an oblique-S_i geometry (Passchier and Trouw 1996), i.e. S_i differs in orientation from S_1 in the wall rock (Fig. 42e). This structure shows that andalusite and cordierite grew intertectonically between D_1 and D_2. A few crystals are indicative of a later age. These porphyroblasts are usually less well bounded and less rotated, demonstrating that porphyroblastesis might have ended during the D_2 event.

Sillimanite grew forming reaction rims along the boundaries of the pre-D_2 andalusite porphyroblasts. In addition, fibrolite commonly shows the effects of D_2 strains. These facts suggest that the prograde substitution of andalusite by sillimanite was mainly syntectonic with D_2 event.

Fig. 42. Microphotographs. (a): S_2 crenulation cleavage defined by the alignment of biotite. PPL. (b): S_2 crenulation cleavage developed only in a pelitic layer. Cleavage domains are made of recrystallized biotite. PPL. (c): Porphyroblasts of cordierite grown over S_1 foliation and containing straight inclusion patterns. CPL. (d): Porphyroblast of garnet grown over $S_{s/1}$ foliation and bearing $S_{s/1}$-parallel inclusions. PPL. (e): Andalusite porphyroblast displaying an oblique-S_i geometry. PPL.

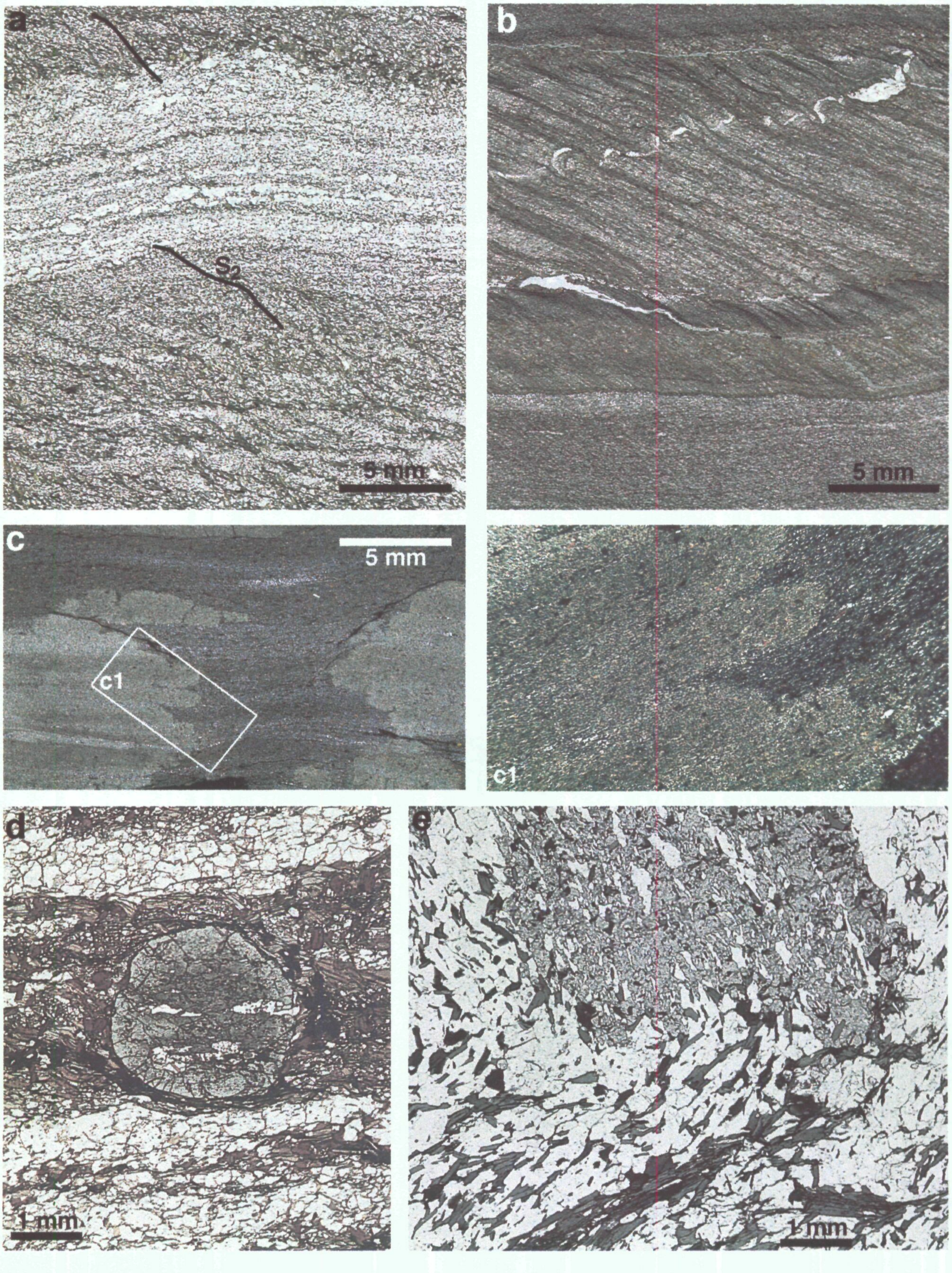
a
S2
5 mm
b
5 mm
c
5 mm
c1
c1
d
1 mm
e
1 mm

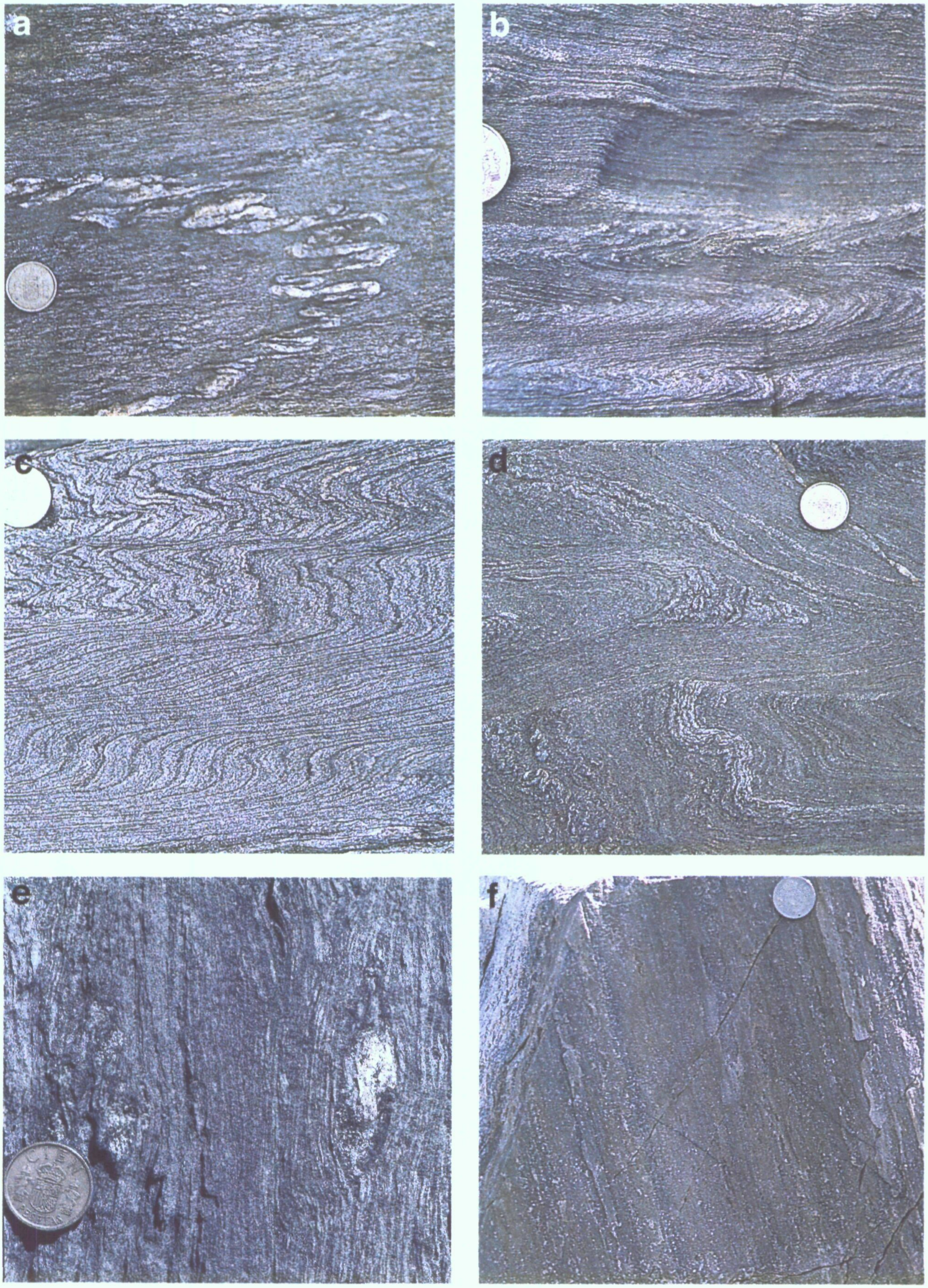

Fig. 43. Photographs of D_2 high strain structures. (a): Tight folds in a quartzitic layer and axial planar S_2 transposition foliation, Tudela. (b): Isoclinal folds and tectonic banding, Rec de Cala Serena. (c): sheared limbs in tight F_2 folds from Cala Prona. (d): Inhomogeneous strain producing highly strained limbs and local disruption, Rec de Cala Serena. (e): Porphyroblast of andalusite wrapped by the S_2 transposition foliation, Cala Cullaró. (f): L_2 stretching lineation in the Culip quartzites.

4.3.2. STRUCTURES IN THE HIGH STRAIN DOMAINS

The Map of Structural Domains shows the present spatial occurrence of D_2-related high strain domains. The larger domain entirely occupies the northern area. Another smaller high strain zone is located in the south slopes of Puig Alt Petit. The high strain domains consist of about ENE-WSW trending sub-vertical zones of tight to isoclinal folds with an axial planar crenulation cleavage (S_2).

The high strain domains are characterized by a low angle between the S_2 crenulation cleavage and S_1 foliation. With increasing D_2 strain, this angle decreases to an average value of about 15-20° (i.e. Tudela zone and SE of Rocal dels Marroquins) and, towards the centre of the high-strain zone, both structural elements become parallel, with the development of isoclinal folds and even a S_2 transposition foliation which replaces S_1 as the dominant foliation (Fig. 43a, b). As a result of this, a nearly ENE-WSW trend of foliations becomes predominant. Folds are close to the class 2 and show sheared limbs (Fig. 43b, c, d). "M"-shaped symmetric folds are common. Inhomogeneous deformation is responsible for the presence, in these high strain domains, of lozenge-shaped zones of less deformation, with relics of S_1 foliation, coexisting with zones of very high strain where S_1 is totally transposed.

A great variety of meso- to microstructures related to the development of the transposition foliation can be observed. In the pelitic layers, tectonic bandings defined by the preferred orientations of micas and/or sillimanite are common. In rocks made of alternances, stretched limbs lead to the isolation of the most competent hinges, becoming rods. Early quartz veins are stretched. Porphyroblasts of cordierite and andalusite appear entirely wrapped by the dominant foliation (Fig. 43e) and they look prekinematic with respect to it, although they are postkinematic with regard to S_1.

Stretching lineations are best developed in these high strain domains (Fig. 43f) and are mainly mineral lineations (micas and sillimanite fibres), or defined by the linear shape of quartz aggregates. Together with other L_2 linear fabric elements such as crenulation lineations and axes of isoclinal F_2 folds, they all plunge moderately (in the western domains) to steeply to the east or to the west (Fig. 37 and Map of Structural domains), although it seems that the stretching lineations have a prevalent west plunging.

The granitoids of the migmatite complexes are located in zones of very high strain. They registered part of D_2 deformation, as these bodies have fold-like shapes and record magmatic to solid state fabrics which are correlatable with the S_2 transposition foliation in the metasediments (explained in section 5.2.).

An example of a D_2 structural setting is shown in detail map and stereographic projections (Fig. 44). This example has been taken from La Birba road zone. It illustrates a sharp transition from low to high D_2 strain domains in medium grade metasediments. In southeastern sub-area, a dominant NE dipping S_1 foliation is folded by late D_3. The northwestern sub-area is a D_2 high strain domain, with a S_2 transposition foliation replacing S_1. Tight to isoclinal folds are abundant in this high strain zone. Stretching lineations in the high strain sub-area and fold axes in both sub-areas are all sub-parallel and moderately east plunging. These structures affect a previous complex tectonic pattern (here interpreted as a steepened thrust) characterized by the presence of the Sant Baldiri complex pinched in between the metasediments.

Microstructures

Microstructures in the high strain domains change considerably in regard to the lower strain domains. All micas display a marked preferred orientation, developing a transposition fabric which can envelop the aluminium silicates and garnets. Cordierite and andalusite porphyroblasts have long axes in the plane of S_2 foliation. Sillimanite fibres, although also adopting a preferred orientation parallel to D_2 fabric, usually display complex folding patterns due to dynamic crystallization (Fig.45a). S_s/S_1 foliation can still be observed in metagreywackes displaying isoclinal folds with axial planar micas (Fig. 45b). An S_2-parallel tectonic banding is most common, with microlithon structures (mainly made of quartz and feldspar grains with granoblastic texture and sometimes including relics of crenulations) and cleavage domains with a high mica content.

Particular microstructures have been observed, for instance, in the black schists outcropping in La

Birba road zone (Fig. 44 and Fig.45c). These rocks show a matrix with a penetrative transposition foliation (S_2), and numerous randomly oriented chloritoid porphyroblasts with inclusion patterns S_i oblique to S_2 in the matrix. Chloritoids are interpreted to be syntectonic with respect to the progressive non-coaxial D_2 deformation.

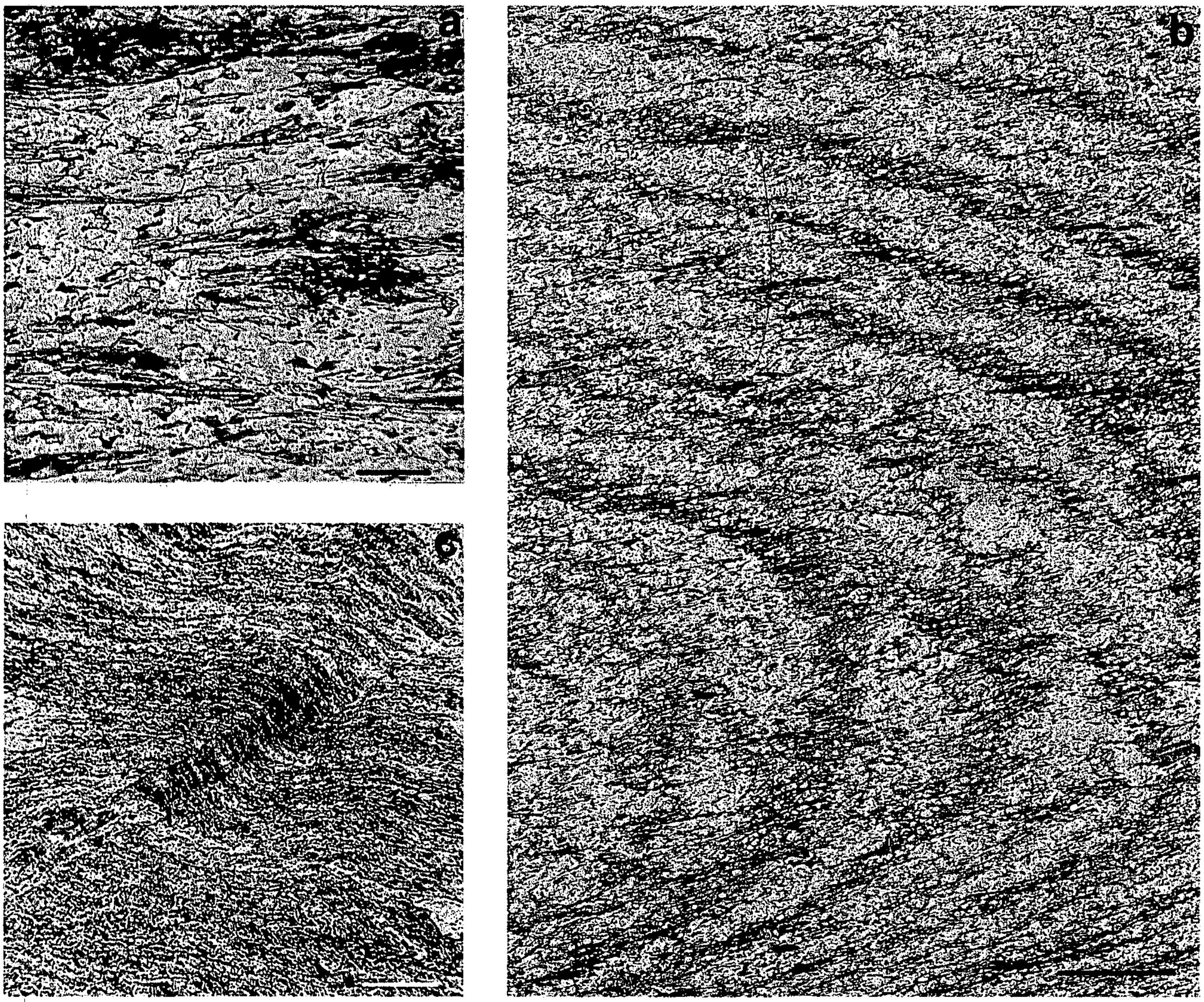

Fig. 45. Photographs of D_2 high strain microstructures. Scale bar = 1 cm. PPL. (a): Transposition foliation defined by preferred orientation of micas and clusters of sillimanite. (b): S2 foliation defined by preferred orientation of biotites parallel to the axial plane of F_2 folds. (c): Chloritoid porphyroblast in a black schist from La Birba road. It is interpreted as syntectonic with respect to the external D_2 foliation.

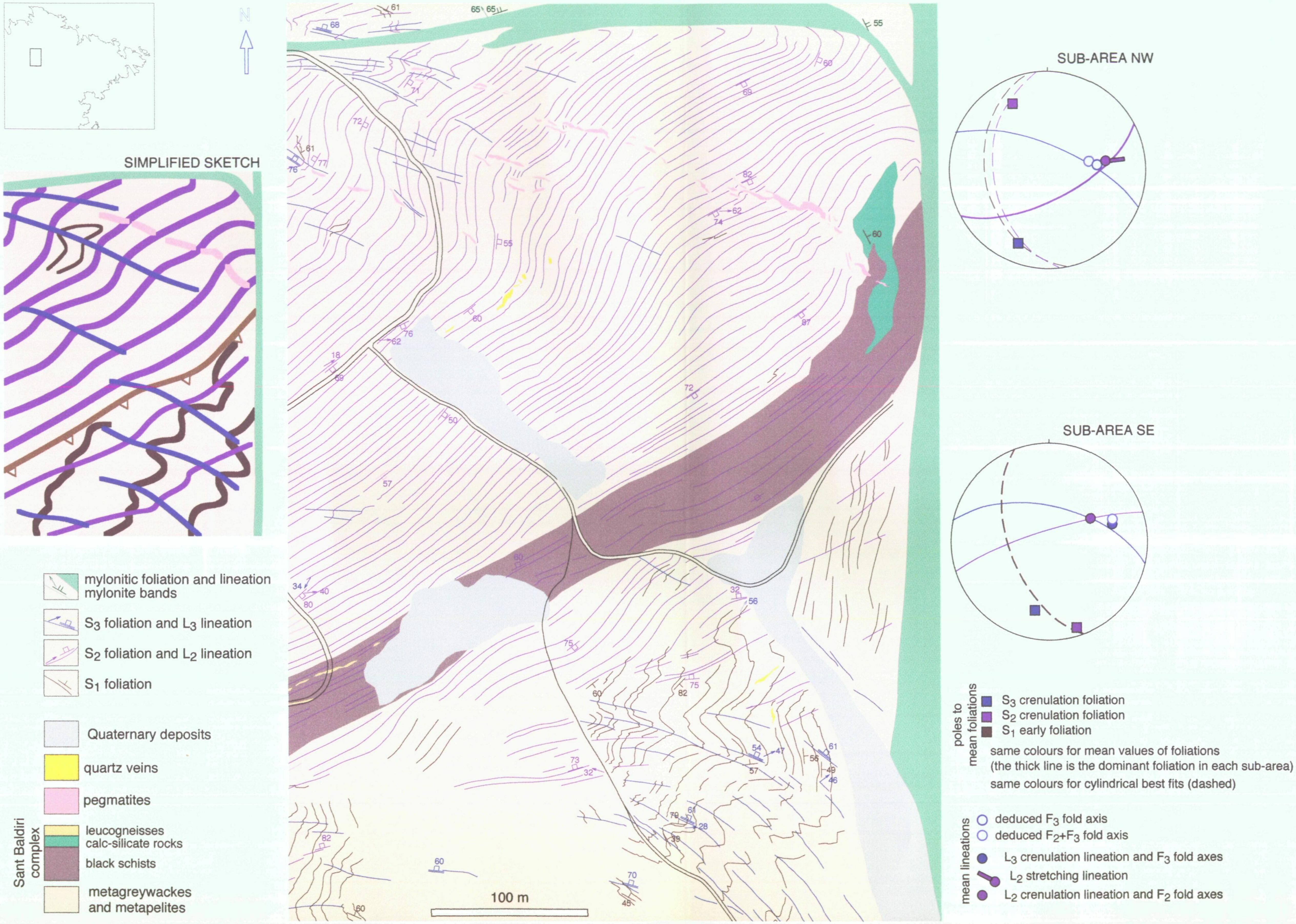

Fig. 44. Structural map of La Birba road zone and equal area lower hemisphere projections of main structural elements of two differentiated sub-areas (NW and SE). In sub-area SE, S_1 is the dominant foliation and it is folded mainly by D_3. S_3 axial planar foliation is more intense than S_2. Sub-area NW is a D_2 high strain domain. S_2 replaces S_1 as the dominant foliation. It is slightly folded by D_3.

4.4. $D_{2\text{-}3}$ E-W FOLDING STAGE

This transitional stage between the D_2 and D_3 events is mainly characterized by the development of folds with sub-vertical E-W-trending axial planes and crenulation cleavages. As previously introduced, this deformational stage took place around the time of the metamorphic peak to high temperature retrogression in the north, but under clear retrograde conditions in the central and southern domains.

In some places, $D_{2\text{-}3}$ deformation led to the development of refolded folds and crenulated crenulations (i.e. Cala Galladera zone), whereas in the majority, a progressive deformational sequence from D_2 to $D_{2\text{-}3}$ gave rise to an unique fold train and associated crenulation cleavage (i.e. Culip-Cap de Creus zone).

4.4.1. PROGRESSION OF D_2 TO $D_{2\text{-}3}$: THE CULIP-CAP DE CREUS EXAMPLE

The Culip-Cap de Creus area (Fig. 46) is an illustrative example of progressive heterogeneous deformation in time and space, with domains of low, medium and high strain affecting medium to high grade metasediments and closely associated to emplacement of pegmatite dykes (Carreras & Druguet 1994a, Druguet et al. 1997). Outcrop is nearly continuous in this ≈ 2 x 1.5 km area, and later overprinting structures are scarce or at least distinctive enough to prevent confusion.

The Culip-Cap de Creus area is located in the medium- to high-grade metamorphic zone, mainly formed by sillimanite-bearing micaschists. In this area, deformation was heterogeneously distributed and three structural domains with relatively high and low strain can be distinguished (Fig. 46). The low strain domains are characterised by a sub-vertical nearly N-S trending $S_{s/1}$. In these domains, D_2 folds are open and the associated crenulations develop exclusively in more pelitic schists. Strain-increase towards the high-strain zone is accompanied by the development of "S"-shaped cylindrical folds in bedding-S_1, on a 10 cm-100 m scale, and associated sub-vertical crenulation cleavage (Fig. 47). These folds have sub-vertical or steeply plunging axes, which are closely parallel to lineations. Most lineations are usually stretching lineations defined by the alignment of quartz grains (linear shape fabric) and mineral lineations defined by sillimanite, tourmaline or biotite. These lineations are mainly developed in the pegmatite dykes, quartz veins and in bedding surfaces.

Earlier boudinaged quartz segregation veins (parallel to S_1) are folded during $D_{2\text{-}3}$, with an anti-clockwise rotation of boudins, systematically located in the short limbs. Porphyroblasts of cordierite or andalusite grown over S_1 are wrapped by the crenulation cleavage and systematically display an anti-clockwise rotation.

Towards the centre of the high strain zone, a further increase in strain is manifested by the increasing tightness of the "S" shaped D_2 folds and the rotation of both $S_{s/1}$ and S_2 towards a steeply dipping NE-SW or even E-W trend. Also, the angle between $S_{s/1}$ and S_2 decreases with increasing strain, from 45° in the low strain areas up to sub-parallelism in the centre of the highest strain zone. The change in orientation of both foliations, from the low strain into the high strain zone, defines a cylindrical sigmoidal structure, with steeply NE plunging axis (Fig. 48). This sigmoidal structure is more developed in the Culip area, having, in horizontal view, an open Z shear zone-like geometry. This pattern is related to strain gradients arisen during the development of folds with E-W axial trace, and intensified by the overprinting of the later D_3 shearing.

In a section across the high-strain zone from southern low-strain zones to the north, the abundance of andalusite porphyroblasts decreases, whereas the density and size of pegmatite dykes and the size of sillimanite grains increases. This suggests that the high strain zone formed at medium to high grade metamorphic conditions, like D_2 structures in the low-strain zones. The change in orientation of S_2 towards the high-strain zone does not appear to be the effect of post-D_2 overprinting, since folds and crenulation cleavages are not disturbed by later deformation phases except in the vicinity of greenschist-facies late shear zones. Thus, leaving aside the late shear zones, it appears that in this area a single high temperature folding event, prior to the shearing event, was responsible for both the sigmoidal pattern and the inhomogeneous distribution of deformation across the area.

This structural pattern is visible at different scales within the low strain domains due to self-similarities, as in examples displayed at metric and microscopical scales (Fig. 49).

Thin layers of Culip-type light quartzites display complex folding structures, specially in low and medium strain domains. A spectrum of differently oriented folds (from NE-SW to E-W) and the presence of multiple fold interference examples, are interpreted in this case as a result of a progressive passage from the D_2 to the D_{2-3} deformation.

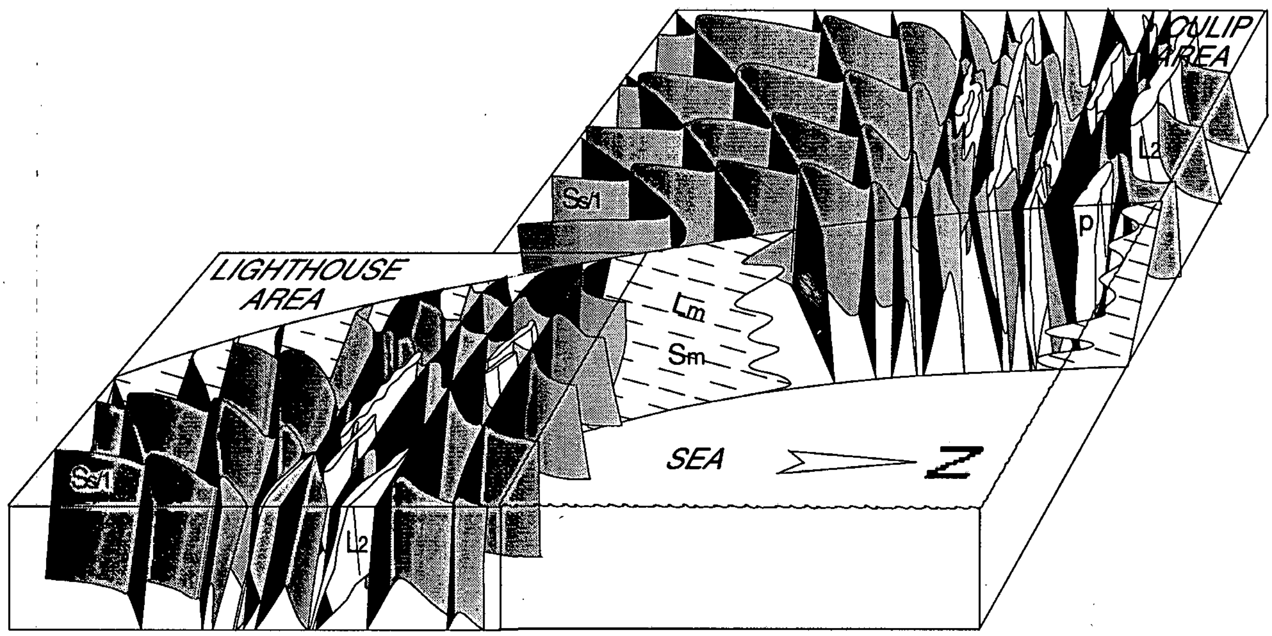

Fig. 47. Schematic block diagram showing the three-dimensional arrangement of the main structural elements in the Culip-Cap de Creus area. For the sake of simplicity, only one late shear zone, separating the Culip and the Lighthouse areas, is represented. $S_{s/1}$: bedding-parallel foliation, S_2: crenulation cleavage, L_2: D_2 related stretching lineation, Sm and Lm: mylonitic foliation and associated stretching lineation, p: pegmatites (after Druguet et al. 1997).

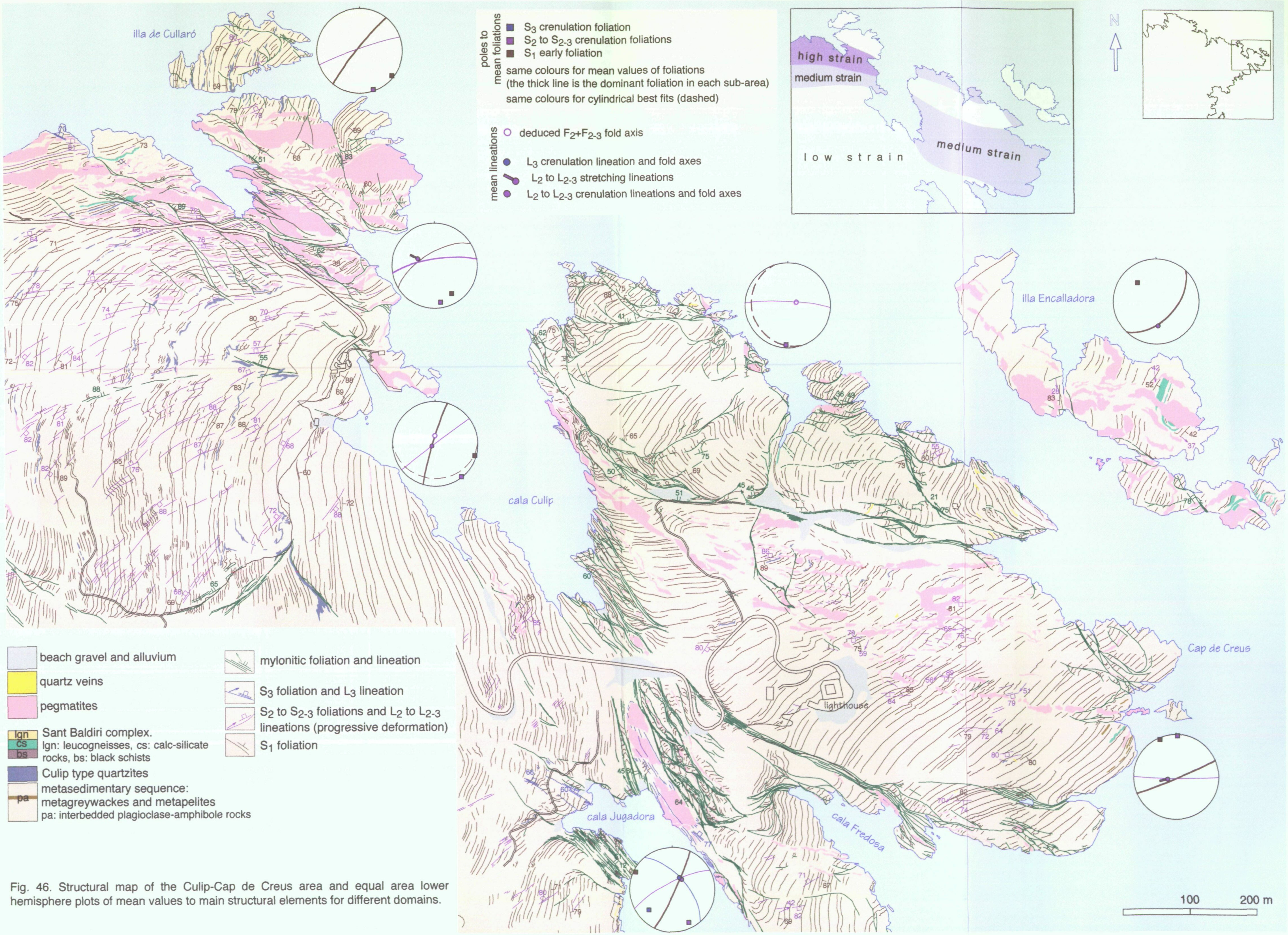

Fig. 46. Structural map of the Culip-Cap de Creus area and equal area lower hemisphere plots of mean values to main structural elements for different domains.

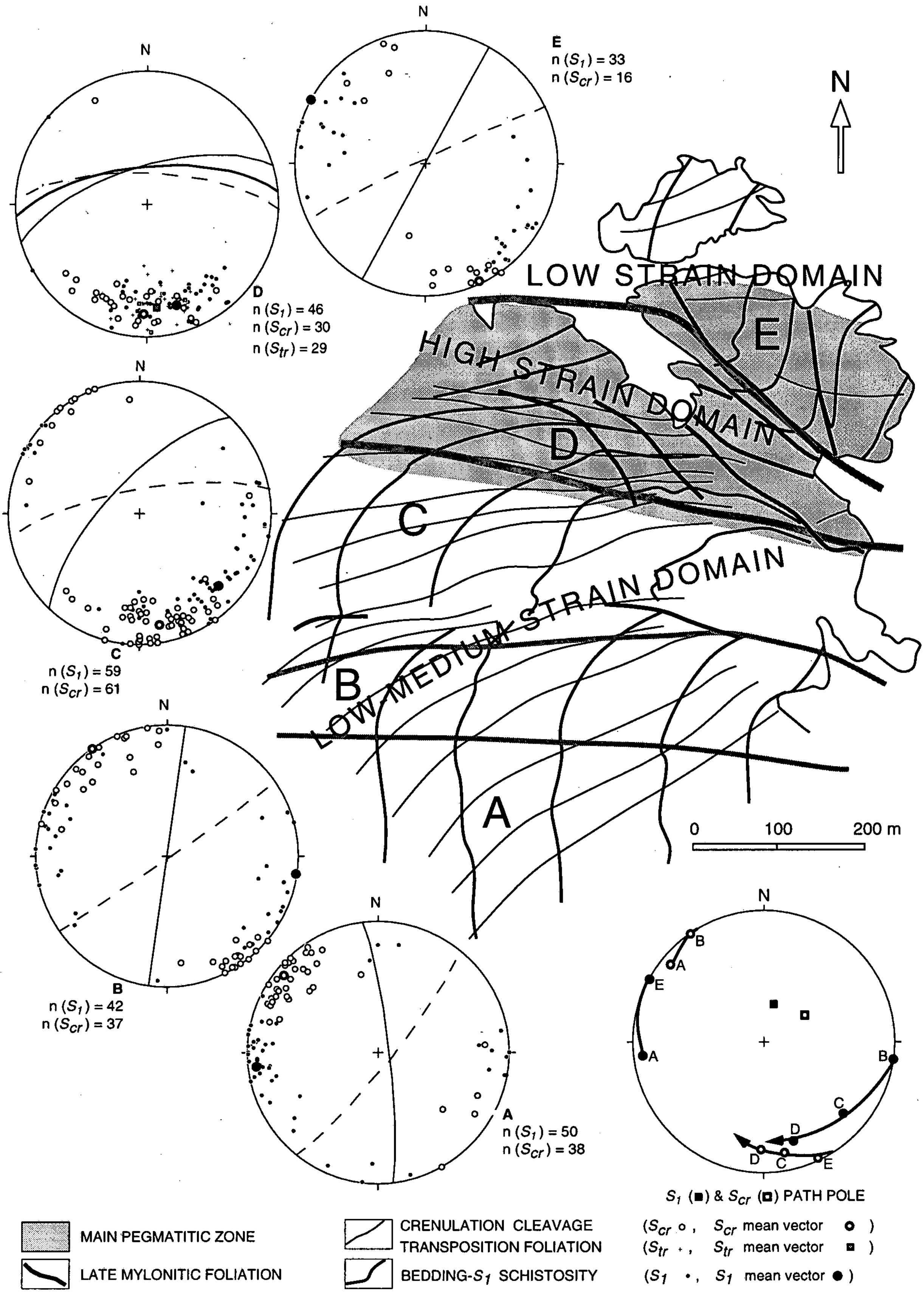

Fig. 48. Equal-area lower-hemisphere projections of the Culip area. In each plot, the great circles represent the main value of S1 (solid) and Scr (dashed) and correspond to each subarea indicated on the map (A-E). In plot "D" the thick solid line corresponds to the main value of the transposition foliation (Str). The pole path projection refers to the clockwise rotation of S1 and Scr. The poles in each path are the main values of each domain. The location of poles of cylindrical best fits of each path are also shown (squares). After Carreras & Druguet (1994a).

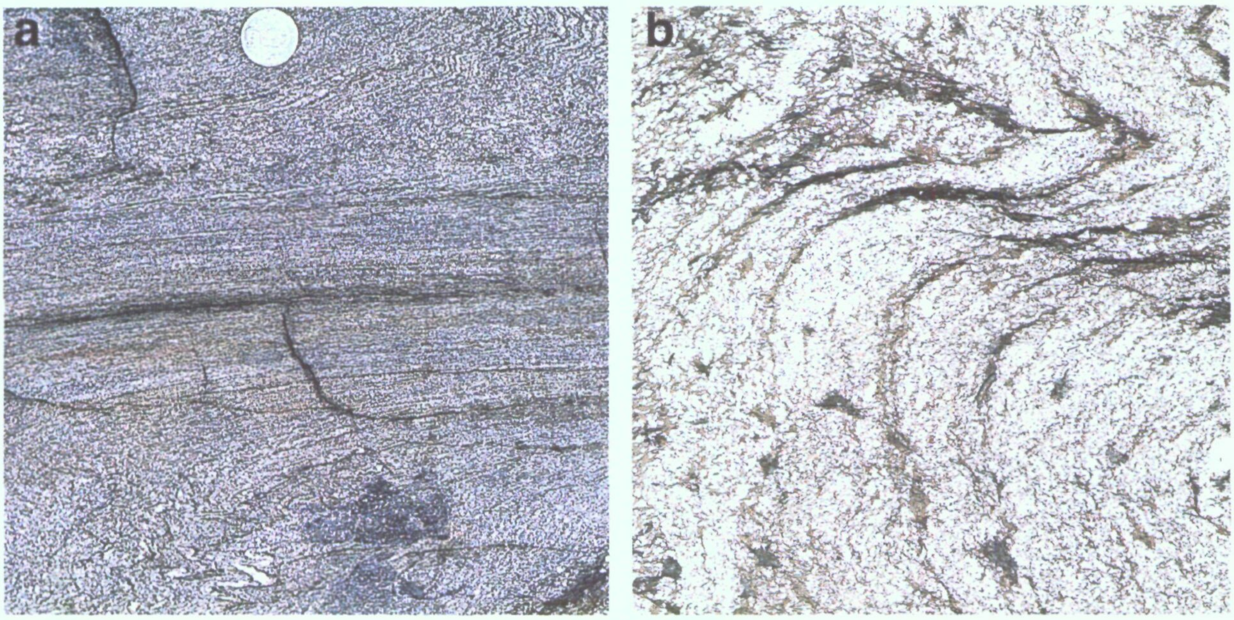

Fig. 49. Structural patterns characterized by the development of zones of relative high and low D_2 to D_{2-3} strain, at the outcrop scale (a: Lighthouse area, horizontal view) and at microscopical scale (b: folded micaschist, Puig de Culip, width of view 2.5 cm, PPL).

4.4.2. OVERPRINTING OF D_2 BY D_{2-3}

The D_{2-3} deformational event is responsible for a few E-W trending hm-scale folds affecting the S_1 and S_2 foliations (Structural Map). Because the S_2 foliation appears folded, a brief period of quiescence or interkinematic lapse might have taken place between D_2 and D_{2-3} folding stages, at least in these domains described below.

THE CANAL GUILLOSA EXAMPLE

The Canal Guillosa area (Fig. 50) is an illustrative example of superposed folding indicated by fold interference patterns in sub-horizontal surfaces. Two different stages of folding have been recognized. The first one corresponds to D_2 folding event at high strains, and the second produced folds with E-W axial traces. This structural sequence affects medium to high grade metasediments and, as in the Culip-Cap de Creus example, it is also closely associated to pegmatite dykes emplacement.

The area comprises isoclinal folds and crenulations affecting bedding and bedding-parallel S_1 foliation, related to the high strain D_2 deformation. The enveloping surfaces of the dominant S_2 axial planar crenulation foliations has a N-S attitude, which is anomalous if compared with the prevalent NE-SW trending S_2 foliation in similar high strain domains (Structural Map). This is the result of post-D_2 local folding.

The upright isoclinal folds and S_2 crenulation foliation are deformed into open folds (Fig. 51) achieving a steeply dipping E-W axial planar crenulation cleavage, selectively developed in the pelitic layers. Occasionally, this second crenulation cleavage evolves to a tectonic banding. Crenulation lineations and axes of E-W folds are sub-vertical, and thus sub-parallel to L_2 and F_2 fold axes. The observed mesoscopic interference patterns at horizontal surfaces closely fit Ramsay (1967) type 3 fold interference pattern, also called refolded folds or convergent-divergent pattern, where the folding is coaxial but the two axial planes are at a high angle. Local deviations in the relative angular relationships between both series of folds give mushroom-like patterns (Fig. 51c), which can also be observed when looking at surfaces oblique to the fold axes.

In Fig. 50, some E-W hectometric open folds affecting the dominant S_2 foliation can be observed, with different asymmetries ("S" and "Z") at each major limb. The changes in the orientation of S_2 defines a cylindrical fold with sub-vertical axis, which is in accordance with the lineations and fold axes measurements.

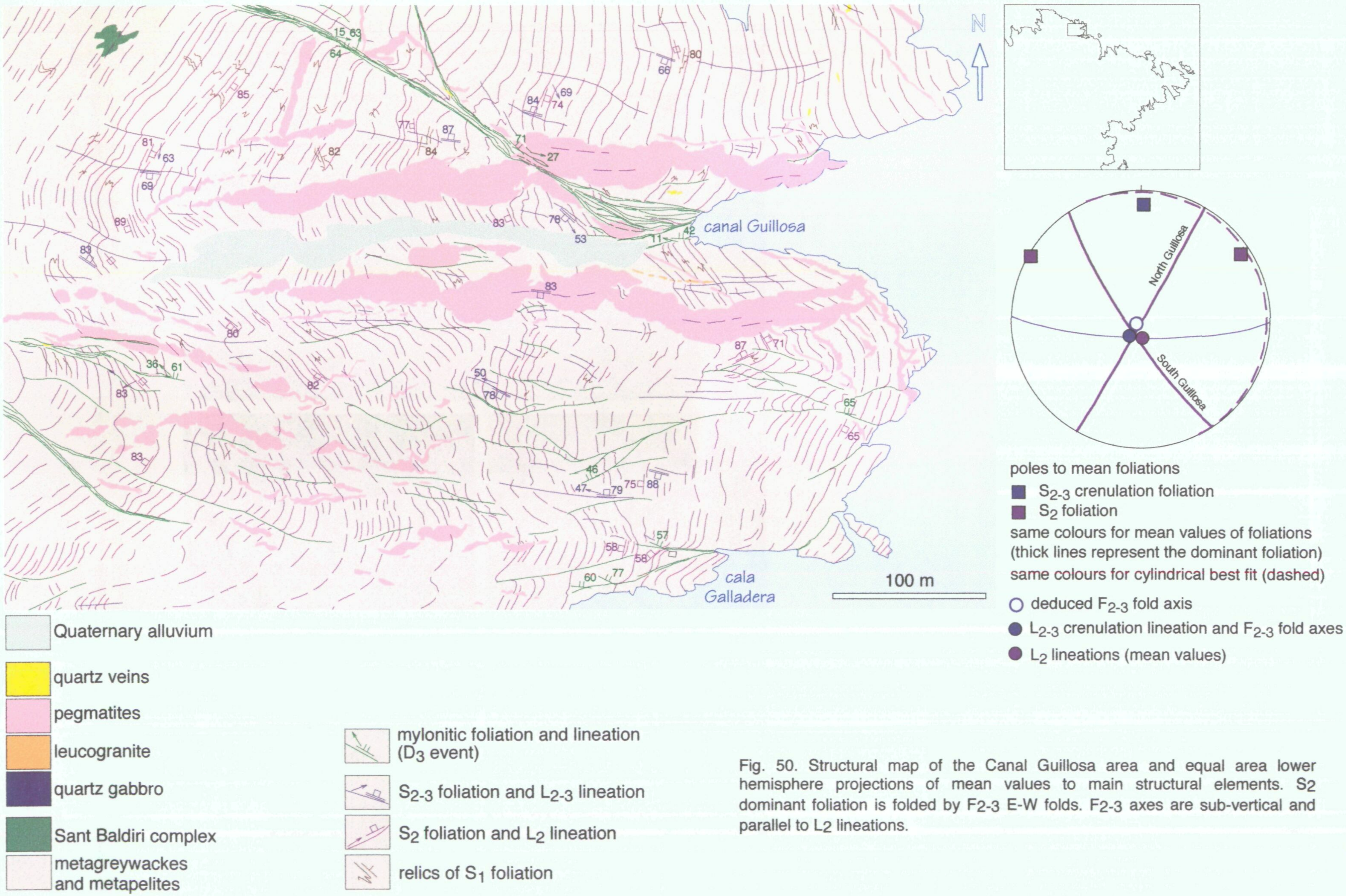

Fig. 50. Structural map of the Canal Guillosa area and equal area lower hemisphere projections of mean values to main structural elements. S_2 dominant foliation is folded by F_{2-3} E-W folds. F_{2-3} axes are sub-vertical and parallel to L_2 lineations.